Nutrition and Cancer
Publication details, including instructions for authors and subscription information:
http://www.tandfonline.com/loi/hnuc20

Suppression by Geraniol of the Growth of A549 Human Lung Adenocarcinoma Cells and Inhibition of the Mevalonate Pathway in Culture and In Vivo: Potential Use in Cancer Chemotherapy

Marianela Galle[a], Rosana Crespo[a], Boris Rodenak Kladniew[a], Sandra Montero Villegas[a], Mónica Polo[a] & Margarita G. de Bravo[a]

[a] Instituto de Investigaciones Bioquímicas de La Plata, Consejo Nacional de Investigaciones Científicas y Técnicas, Centro Científico Tecnológico, Universidad Nacional de La Plata, Facultad de Cs. Médicas, La Plata, Argentina

Published online: 29 May 2014.

To cite this article: Marianela Galle, Rosana Crespo, Boris Rodenak Kladniew, Sandra Montero Villegas, Mónica Polo & Margarita G. de Bravo (2014): Suppression by Geraniol of the Growth of A549 Human Lung Adenocarcinoma Cells and Inhibition of the Mevalonate Pathway in Culture and In Vivo: Potential Use in Cancer Chemotherapy, Nutrition and Cancer, DOI: 10.1080/01635581.2014.916320

To link to this article: http://dx.doi.org/10.1080/01635581.2014.916320

Nutrition and Cancer, 1–8, 2014

ISSN: 0163-5581 print / 1532-7914 online
DOI: 10.1080/01635581.2014.916320

Routledge
Taylor & Francis Group

Suppression by Geraniol of the Growth of A549 Human Lung Adenocarcinoma Cells and Inhibition of the Mevalonate Pathway in Culture and In Vivo: Potential Use in Cancer Chemotherapy

Marianela Galle, Rosana Crespo, Boris Rodenak Kladniew, Sandra Montero Villegas, Mónica Polo, and Margarita G. de Bravo

Instituto de Investigaciones Bioquímicas de La Plata, Consejo Nacional de Investigaciones Científicas y Técnicas, Centro Científico Tecnológico, Universidad Nacional de La Plata, Facultad de Cs. Médicas, La Plata, Argentina

Geraniol (G)—a natural compound present in the essential oils of many aromatic plants—has attracted interest for its potential antitumor effects. The molecular mechanisms of the growth inhibition and apoptosis induced by G in cancer cells, however, remain unclear. In this study, we investigated the effects of G on cell proliferation in culture in A549 cells and in vivo in those same tumor cells implanted in nude mice fed diets supplemented with 25, 50, and 75 mmol G/kg. We demonstrated that G caused a dose- and time-dependent growth inhibition of A549 cells and tumor growth in vivo along with an induction of apoptosis. Moreover, further in vivo assays indicated that G decreased the levels of 3-hydroxymethylglutarylcoenzyme-A reductase—the rate-limiting enzyme in cholesterogenesis—in a dose-dependent manner along with cholesterogenesis and cholesterolemia in addition to reducing the amount of membrane-bound Ras protein. These results showed that the doses of G used in this work, though nontoxic to animals, clearly inhibited the mevalonate pathway, which is closely linked to cell proliferation and increased apoptosis in A549 tumors, but not in normal mouse-liver cells. Accordingly, we suggest that G displays significant antitumor activity and should be a promising candidate for cancer chemotherapy.

INTRODUCTION

Over the past decade, lung cancer—one of the most common causes of death from malignancy in the world—caused 1.37 million deaths per year worldwide (1). Nonsmall-cell lung cancer accounts for over 80% of newly diagnosed lung cancer with the majority of patients being diagnosed with advanced and unresectable disease (2). For our studies we selected the A549 cell line because of its derivation from a typically malignant and invasive nonsmall-cell lung carcinoma. As cells that are actively proliferating, the A549 line requires at least 2 products from the mevalonate pathway: cholesterol and certain nonsterol products (3). The major rate-limiting enzyme in cholesterol biosynthesis in mammalian cells is 3-hydroxymethylglutarylcoenzyme-A reductase (HMGCR) catalyzing the synthesis of mevalonic acid—a precursor for isoprenoid intermediates that are subsequently incorporated into various end-products, including cholesterol plus farnesylated and geranylgeranylated proteins (3,4). Cancer cells rapidly proliferate and may thus require an increased concentration of all these products for optimal cell growth. A greater demand for cholesterol can be by an increased HMGCR activity and/or an enhanced extracellular cholesterol uptake via the low-density-lipoprotein receptor (5). Although an elevated HMGCR activity has been found to commonly occur in tumors along with a resistance to the transcriptional feedback regulation by sterols, isoprenoids could still act to mediate an inhibition posttranscriptionally (6–8). A modified rate of synthesis of nonsterol compounds could also increase isoprenylated proteins. Protein isoprenylation within the cell results in a localization of small GTPases in cellular membranes (9). These proteins are also involved in signal transduction, cellular growth control, and apoptosis. The Ras protein is the most extensively studied small GTPase. The presence of a Ras mutation in the cell has been associated with malignancy, thus making the membrane-localized Ras a rational target for anticancer therapy. Nonmembrane-localized Ras, however (mutated or not) is generally mitogenically inactive (4).

Plant isoprenoids—a broad class of plant products derived from the mevalonate pathway—are recognized as potent suppressors of mammalian HMGCR. Although some of those

Submitted 25 June 2013; accepted in final form 10 March 2014.

Address correspondence to Marianela Galle, INIBIOLP (CONICET, CCT La Plata – UNLP), Facultad de Cs. Médicas, Calles 60 y 120, La Plata, Argentina. Phone: +54 221 4824894. Fax: +54 221 4258988. E-mail: mgalle@med.unlp.edu.ar

studies demonstrated that plant-derived isoprenoids decreased the amount of enzyme, the specific levels at which this regulation occurs have not yet been well characterized (10). Moreover, these natural products showed significant antitumor activity in a variety of cells in culture and are therefore emerging as potent anticancer agents in cancer chemotherapy and chemoprevention (8,11,12).

Geraniol (G) (3,7-dimethylocta-trans-2,6-dien-1-ol), an acyclic monoterpene alcohol of empirical formula $C_{10}H_{18}O$, is a common constituent of several essential oils and occurs in *Monardafistulosa* (<95.0%), ninde oil (66.0%), rose oil (44.4%), palmarosa oil (53.5%), and citronellaoil (24.8%) (13).

The aim of this work was therefore to study the effects of G on A549 cells—here to be used as a model for human pulmonary carcinoma—both in culture and in athymic mice bearing those A549 cells as a tumor in vivo to shed light on the mechanisms by which G could exert antitumor activity as well as to determine the relationship between growth control and the regulation of the mevalonate pathway.

MATERIALS AND METHODS

Reagents

G (98%) was supplied by Sigma (St. Louis, MO). The inorganic reagents and solvents were of analytical grade and obtained from Merck (Darmstadt, Germany), Analyticals Carlo Erba (Milan, Italy), and Sigma (St. Louis, MO). [^{14}C]acetate (54.7 Ci/mol) was purchased from Perkin Elmer Life Sciences, Inc. (Boston, MA).

Cultured Cells

The nonsmall-cell human pulmonary-carcinoma cell line A549 was obtained from Dr. Amada Segal-Eiras (CINIBA, UNLP. Argentina). The cells were maintained in 75-cm^2 tissue-culture flasks in Eagle's Minimal Essential Medium (MEM) (Gibco, Invitrogen, Carlsbad, CA) supplemented with 10% (v/v) (Natocor, Córdoba, Argentina) fetal-bovine serum and 100 μg/ml streptomycin that had been filter-sterilized. The cells were routinely grown at 37°C in a humidified atmosphere with 5% (v/v) CO_2 in air. For the assays and the continuous cell propagation, surface cultures in exponential growth (at about 80% confluence) were harvested with 0.25% (w/v) trypsin in phosphate-buffered saline (PBS; 1.5 mM KH_2PO_4, 8.1 mM $Na_2HPO_4.2H_2O$, 0.14 M, NaCl, 2.7 mM KCl, pH 7.4). Cell proliferation was measured by the MTT assay (14). For the assay A549 cells were seeded in 24-well plates at 8×10^3/well, and the cultures kept at 37°C for 24 h for cell attachment before further additions. The cells were then incubated with G for 24 h, with the added G having been dissolved in a volume of dimethylsulfoxide (DMSO) such that the final concentration of that vehicle was 0.05% (v/v). That same concentration of DMSO was therefore added in parallel to the control cultures. After treatment, the cells were incubated with 0.5 mg/ml of [3-(4,5-dimethylthiazol-2-yl)-2,5-diphenyltetrazolium bromide (MTT; Sigma Chemical Co., St Louis, MO)] in PBS at 37°C for 2 h. The MTT was then removed from the wells and acidified with 0.04 M HCl in isopropanol. The absorbance of the reaction product (the formazan) was measured at 560 nm with background subtraction at 640 nm with a Beckman Coulter DTX 880 Microplate Reader.

Tumor Tissue

A549 cells were detached, centrifuged, resuspended in MEM, and implanted subcutaneously in the back of nude mice (2×10^6 cells/mouse). Tumor growth was evident between 15–20 days following inoculation. Tumors weighing between 2–3 g were transplanted as described by Polo and Bravo (15) to reduce the lag time and minimize both the variables *lag time* and *growth rate* in all the implanted tumors. The procedure stated in brief: Tumors were surgically removed and washed with MEM, the necrotic regions eliminated and the remaining tissue cut and dispersed by passage through a 1-mm^2 steel mesh to obtain a tissue suspension of 300 mg/ml. Finally, each animal was inoculated subcutaneously with 0.2 ml of that suspension. Tumors were measured twice a week with calipers and their volume calculated for an ellipsoid by the formula $V = a^2 \times b/2$, where a is the width and b is the length of the mass.

Animals and Diets

NIH female mice bearing the nu/nu genotype were obtained from the Bioterio of Centro Atómico Ezeiza and housed in a temperature-controlled room on a 12-h cycle of light and darkness. The host animals were maintained ad libitum on a gamma-irradiated chow diet and autoclaved water until the average tumor size reached 300 mm^3. The mice were then randomly separated into 1 control group and 3 test groups. The latter received supplemented diets containing 25, 50, and 75 mmol G/kg food, whereby the animals accordingly ingested 0.099 ± 0.006, 0.201 ± 0.0125, 0.291 ± 0.017 mmol G/mouse/day, respectively. After 3 weeks of treatment all the mice were injected with [^{14}C]acetate (25 μCi/animal) and 3 h thereafter killed at the mid-light period. Blood was collected and serum cholesterol determined by means of a commercial kit (Wiener, Rosario, Argentina). Livers and tumors were immediately removed, minced into pieces, placed into cold buffer solution, and processed as indicated below. All experiments on animals were done in conformity with the Handbook of Laboratory Animal Management and Welfare (16). The animal-use protocols used were approved by the Institutional Animal Care and Use Committee, Facultad de Ciencias Medicas, Universidad Nacional de La Plata, Protocol number 04-001-13.

Lipid Extraction and Analysis

Lipids from mouse liver, tumors, and A549 cells were extracted with chloroform:methanol (2:1 v/v) (17) and

saponified with 10% (w/v) KOH in methanol at 85°C for 45 min. Nonsaponifiable lipids were extracted with petroleum ether. Radioactivity incorporation into nonsaponifiable lipids or cholesterol was measured in a Wallac 1214 Rackbeta liquid-scintillation counter (Pharmacia, Turku, Finland) at 97% efficiency for [^{14}C]cholesterol.

Western Blotting

To determine HMGCR and total Ras (both membrane-bound and cytosolic) levels, small pieces of liver tissue and/or tumor (0.3 g) were homogenized in a buffer solution (10 mM HEPES, pH 7.9; 10 mM KCI; 0.1 mM ethylenediaminetetraacetic acid (EDTA); 0.1 mM ethylene glycol tetraacetic acid; 1 mM dithiothreitol; 0.5 mM phenylmethanesulfonylfluoride). To determine the Ras levels in the plasma membranes of the tumor cells, that subcellular fraction was obtained after Mander et al. (18), but with modifications: Tumor tissue was homogenized in buffer (10 mM HEPES, 0.25 Msacarose, 1 mM EDTA, pH 7.4) and centrifuged at 16,000 × *g* for 15 min. A Nicodenz-Ficoll gradient (1–22%) was prepared in the laboratory. The supernatant of the tumor sample was loaded onto the gradient and sedimented in an L8.70M ultracentrifuge at 230,000 × *g*, in a SW60 Ti rotor (Beckman Coulter, Fullerton, CA) at 4°C for 16 h. Fractions were collected from the top of the gradient. The protein content in each sample was assayed by the Bradford method (19) with Coomassie brilliant blue G-250 and bovine-serum albumin as standard. Liver and tumor proteins were boiled in sample buffer supplemented with 5% (v/v) ß-mercaptoethanol for 5 min. The samples were electrophoresed on 12.5% (w/v) sodiumdodecylsulfide polyacrylamide gels and adsorbed to polyvinylidene difluoride (PVDF) membranes (Amersham, GE Healthcare, Little Chalfont, UK) by semidry transfer at 10 V for 1 h in 48 mM Tris pH 8.3, 39 mM glycine containing 20% (v/v) methanol. Nonspecific protein-binding sites were blocked by incubation in PBS containing 0.05% (v/v) Tween 20 and 5% (v/v) skimmed milk. The membrane was incubated with anti-HMGCR (Santa Cruz Biotechnology, Santa Cruz, CA) or anti-pan-Ras antibody (Calbiochem, Darmstadt, Germany) diluted 1/200 in antibody-dilution buffer [2% (v/v) skimmed milk in PBS plus 0.1% (v/v) Tween 20] for 1 h followed by three 5-min washes in the same buffer. Horseradish-peroxidase-conjugated antibodies (Santa Cruz Biotechnology, Santa Cruz, CA) were added to the membrane for 1 h. Internal control was loaded with anti-ß-actin antibody (Sigma, St. Louis, MO). Immunoreactive bands were detected by enhanced-chemiluminescence Western-blot–detection reagents (Amersham Pharmacia Biotech, Little Chalfont, UK) and processed manually through the use of common X-ray film developers and fixers. Protein immunoblots were scanned and the density of each band quantified by means of the ImageJ software (Image processing and analysis in Java). As an internal control, PVDF membranes probed for plasma-membrane-associated Ras were stained with Coomassie brilliant blue R 250.

Apoptosis-Detection System

TUNEL Assay

Tumor tissues were fixed in 10% (v/v) buffered formaldehyde. For apoptosis quantification, the tissue sections were processed for in-situ immunohistochemical localization of nuclei exhibiting DNA fragmentation by the technique of terminal deoxynucleotidyl-transferase- (TdT-)mediated dUTP–TMR-red nick-end labelling (TUNEL) with the In-Situ Cell Death Detection Kit (TMR Red, Roche, Mannheim, Germany). Sections were treated according to the manufacturer's instructions and as described by Meresman et al. (20). The method stated in brief: Sections were deparaffinized, rehydrated with xylene and ethanol, permeabilized with 20 g/mL proteinase K (Invitrogen, Carlsbad, CA), rinsed with PBS, and finally immersed in the TdT buffer provided by the kit containing the labelled nucleotides and incubated at 37 °C for 1 h. The TUNEL-positive cells were evaluated under an Olympus BX51 fluorescence microscope (Tokyo, Japan) equipped with an Olympus DP70 digital camera and the results analyzed through the use of the ImagePro Plus v5.1 software (Media Cynernetics, Silver Spring, MD). The data were expressed as the percentage of TUNEL-positive cells relative to the total number of cells, the latter being determined by uptake of the fluorescent dye DAPI (4', 6-diamidino-2-phenylindole dihydrochloride; Invitrogen by Life Technologies, Carlsbad, CA).

Caspase-3 Activity

Tumor caspase-3 activity was determined by the Caspase-3 Assay Kit, Colorimetric (Sigma, St. Louis, MO) according to the manufacturer's protocol but adapted for measuring tissue as follows: The tissue homogenate was obtained with 200 mg of tissue in 300 μL of lysis buffer provided by the kit. The reaction mixture for 96-well–plate microassay with 100 μl of final volume contained 5 μl of tissue homogenate along with 10 μL of the caspase-3 substrate: acetyl-Asp-Glu-Val-Asp-p-nitroanilide (2 mM) added to 85 μL of the assay buffer included in the kit. The p-nitroaniline moiety released from the substrate by caspase-3 was measured at 405 nm with a Beckman Coulter DTX 880 Microplate Reader. The concentration of the p-nitroaniline was calculated from a calibration curve prepared with defined p-nitroaniline solutions.

Statistical Analysis

The results are expressed as the means ± SEM, and all analyses were conducted with GraphPad InStat 3.0. Statistical differences between the control and the G-treated cells or animals were evaluated by the analysis of variance test followed by Tukey HSD post-hoc comparisons. Differences were considered significant at a $P < 0.05$.

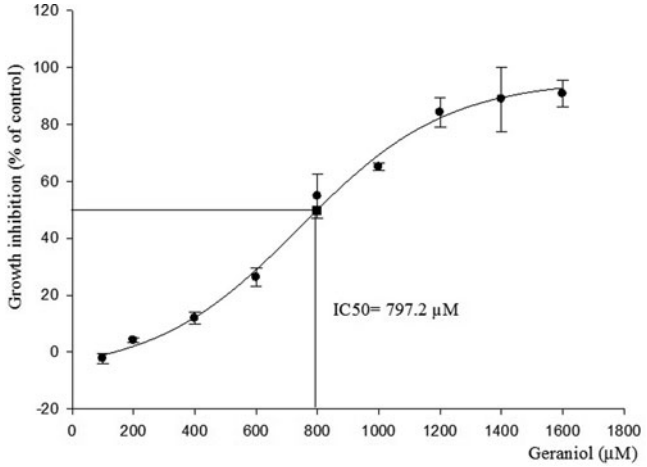

FIG. 1. Dose–response curve of A549 cells incubated with geraniol, expressed as percent inhibition of cell growth as assessed by the MTT test. Each point on the curve was calculated from the mean value ± SD of 8 replicate wells per dose performed in 3 separate experiments.

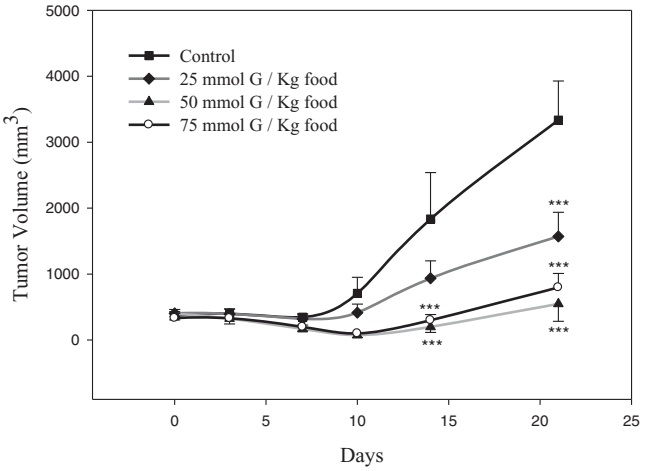

FIG. 2. The effect of geraniol on tumor volume. A549 cells were implanted subcutaneously in the back of nude mice (2×10^6 cells/mouse). Animals bearing tumors of approximately 300 mm^3 received supplemented diets containing 0, 25, 50, and 75 mmol G/kg diet. Tumors were measured twice a week with calipers and the volume calculated as an ellipsoid through the formula $V = a^2 \times b/2$, where a is the width and b is the length. The data are presented as means ± SEM for each group. $^{***}P < 0.001$ vs. control.

RESULTS

Inhibition by G of A549-Cell Proliferation in Culture

The effects of G were first tested on the A549 cell line in culture. Dose-response studies on cell proliferation were conducted with 0–1,800 μM G (Fig. 1). The IC50 value for G, determined from the graph depicted in Fig. 1, was 797.2 μM.

Tumor-Growth Suppression by Geraniol

The data obtained from measurement of tumor volume in A549-bearing mice twice a week for 21 days (Fig. 2) demonstrated that G significantly decreased tumor growth from Day 14 in the groups receiving 50 and 75 mmol G/kg food. For the group receiving a lowest dose (25 mmol G/kg food), the reduction in tumor size became significant only at the end of the treatment.

The inhibition of tumor growth by G was also demonstrated by the tumor-weight data obtained (Table 1). Although the decrease in tumor weight in the mice treated with the lowest dose of G was not statistically significant, the inhibition of tumor growth at the 2 higher doses evaluated was highly significant. No difference in the body or liver weight ($P > 0.05$) was observed between the different experimental groups: Thus, G caused no apparent toxicity at the dosages that were used.

The Effect of G on RAS-Protein Levels

Western blot analysis indicated that G treatment of the tumor-bearing mice at the intermediate dose (50 and mmol G/kg food) resulted in a decrease in the level of membrane-bound Ras protein in the tumors compared to controls, whereas the total Ras-protein levels did not vary significantly in any of the G-treated groups (Fig. 3).

Increase in Apoptosis in the Tumor Cells After G Treatment

Apoptosis in tumor cells was evaluated by the TUNEL assay and by caspase-3 activity (Fig. 4). We observed comparable results with those 2 different methods. At the higher doses the isoprenoid significantly enhanced apoptosis. Nevertheless, there were no significant differences between 50 and 75 mmol G/kg food: Mice treated with 50 mmol G/kg food, however, showed a somewhat greater percentage of tumor-cell death.

Cholesterolemia and Cholesterogenesis

To determine the influence of G on circulating cholesterol, we measured the total serum cholesterol in each mouse. The results demonstrated that serum cholesterol became significantly decreased at the higher doses of G (Table 2). We also evaluated the effect of G on cholesterol synthesis in liver and in the tumor cells and determined the extent of the

TABLE 1
The effect of geraniol on tumor growth and liver and body weights

Group	Tumor weight (g)	Body weight (g)	Liver weight (g)
Control	2.64 ± 0.73	21.67 ± 0.27	1.68 ± 0.10
25 mmol G/kg food	1.57 ± 0.36	23.49 ± 0.60	1.86 ± 0.11
50 mmol G/kg food	0.55 ± 0.26*	21.98 ± 0.94	1.75 ± 0.07
75 mmol G/kg food	0.79 ± 0.21*	20.70 ± 0.64	1.72 ± 0.07

The values represent the means ± SEM, $n = 5$. Difference is statistically significant relative to the controls at (*) $P < 0.05$.

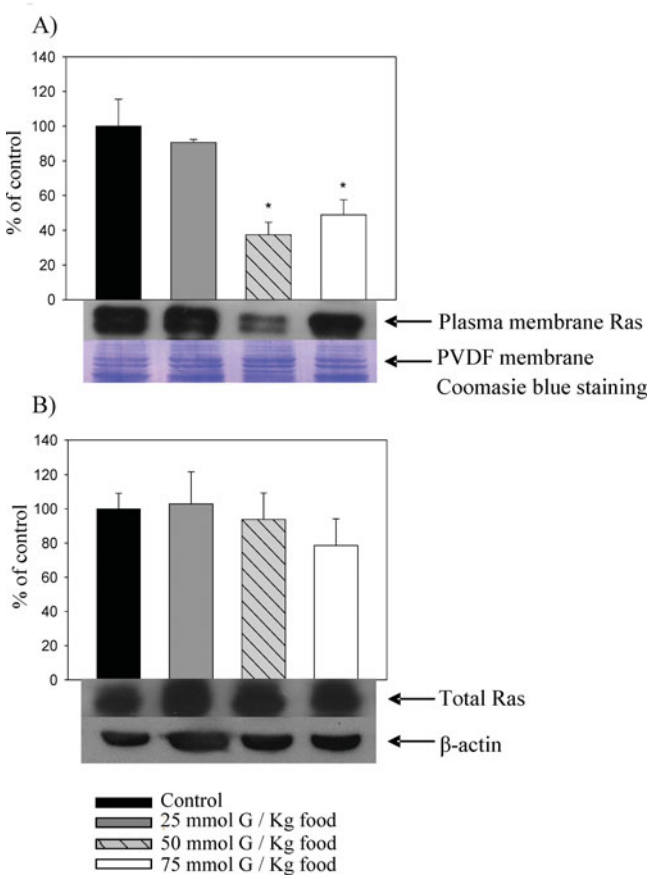

FIG. 3. The effect of geraniol on the levels of total and membrane-bound Ras by Western blot analysis. A: Western blot analysis of plasma-membrane-bound Ras was performed with plasma-membrane fractions obtained from the tumors of 3 individual mice per group (0, 25, 50, and 75 mmol G/kg food). Upper panel: Density of Ras-immunoblot bands as a percent of the control after scanning and correction for differences in loading as described in **Materials and Methods**. Middle panel: Ras-immunoblot bands. Lower panel: Polyvinylidene-difluoride (PVDF) membrane stained with Coomasie blue as a loading control. B: Western-blot analysis of total Ras was performed with tumor homogenate obtained from 3 individual mice per group (0, 25, 50, and 75 mmol G/kg food). To confirm the equal loading of protein samples, membrane was incubated with β-actin. Upper panel: Density of Ras-immunoblot bands as a percent of the control after scanning as described in **Materials and Methods**. Middle panel: Ras-immunoblot bands. Lower panel: ß-actin–immunoblot bands. Values are expressed as means ± SEM. $^*P < 0.05$ vs. control group (color figure available online).

conversion of [^{14}C]acetate into cholesterol and other non-saponifiable lipids by quantification of the incorporation of radioactivity into that fraction after 3 h. In vitro assays furthermore indicated that cholesterol synthesis was significantly reduced by 55% in A549 cells incubated with 200 μM G compared to controls (29 ± 7 *vs.* 13 ± 4 dpm/μg cellular protein). In in vivo assays we found that the radioactivity incorporation was significantly reduced in the livers and tumor cells of mice treated with 75 mmol G/kg food, whereas in mice treated with 25 and 50 mmol G/kg food the decrease was not statistically significant (Table 2).

Decreases in HMGCR Protein Levels After G Treatment

To determine the molecular mechanism by which the mevalonate pathway was affected by G, we measured by Western blot analysis the levels of HMGCR protein in both the mouse-host livers and the A549 tumors (Fig. 5). Our data demonstrated that G decreased HMGCR levels in both tissues in a dose-dependent manner.

DISCUSSION

The potential use of natural products as antineoplastic drugs is nowadays a topic of increasing interest in human medical investigation. Plant isoprenoids have been suggested as suppressing the growth of cancer cells and tumor development through multiple effects on the mevalonate pathway (8). The molecular mechanisms underlying these actions, however, remain poorly understood. Recent studies demonstrated that G had significant antitumor activity in a variety of cell-culture systems representative of liver, colon, pancreatic, and skin cancers (21–24). In addition, the findings from the present study constitute the first indications of the antiproliferative effect of G on human lung adenocarcinoma cells as exemplified in the A549 line. Here, we demonstrated that G inhibits A549-cell proliferation both in culture (Fig. 1) and in vivo (Fig. 2). These results are consistent with the antitumor activity of G against murine hepatomas (23,25). That most of those in vivo studies, however, suggested that G exerts a chemopreventive but not a chemotherapeutic action is noteworthy (25,26). In this work we demonstrated that dietary G effectively inhibits tumor growth in mice when administered following tumor appearance, thus documenting the isoprenoid's effectiveness as a chemotherapeutic agent. Tumor cells in mice treated with higher doses of G (50 and 75 mmol G/kg food) exhibited a lower growth rate than in the absence of G (Fig. 2, Table 1). That the tumor-growth kinetics in the mice treated with those 2 doses of G did not differ significantly suggested that 50 mmol G/kg food could be provisionally considered to produce the maxim tumor growth inhibition attainable (i.e., the effect reaches a plateau at that dosage).

We recently reported that G inhibited the mevalonate pathway at several levels and depressed cell growth in the human hepatoma cell line Hep G2 (27–29). The relevance of the present work resides in the finding that G likewise inhibits the mevalonate pathway in human lung cancer cells in vivo as well as in normal mouse-liver cells, as shown by the decrease in nonsaponifiable-lipid synthesis (Table 2) and the decline in HMGCR levels (Fig. 5). Moreover, our studies indicated that G inhibited cell proliferation in A549 cells both in culture (Fig. 1) and in vivo (Fig. 2) and furthermore decreased the level of membrane-bound Ras protein (Fig. 3). To obtain full oncogenic potency, the Ras protein attaches to the inner plasma membrane in a process mediated by prenyl groups. Farnesyl pyrophosphate and geranylgeranyl pyrophosphate are the

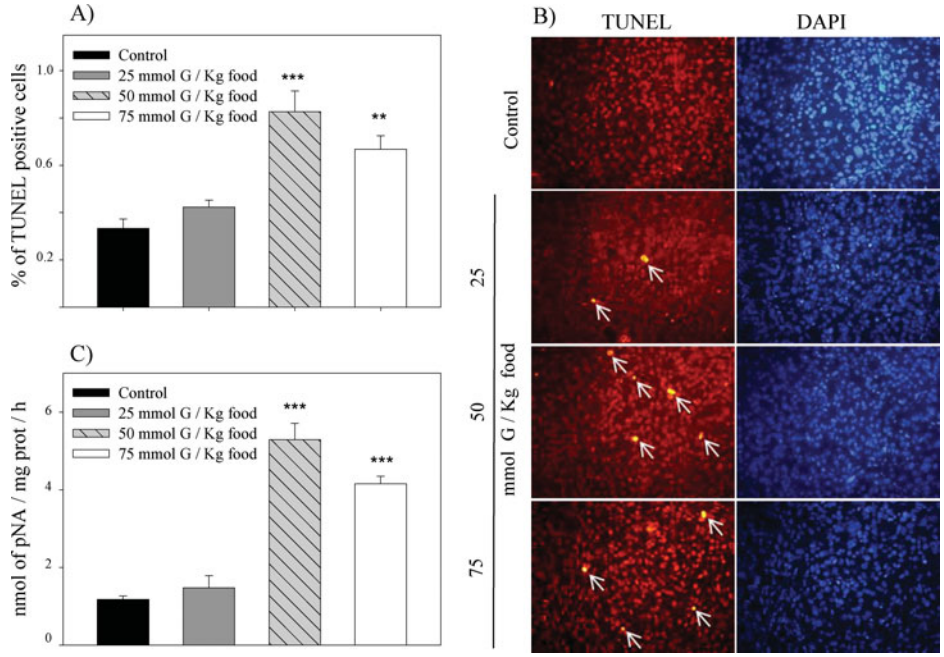

FIG. 4. Apoptosis detection. A: The percentage of apoptotic cells in tumor histological sections were determined by the TUNEL assay. The TUNEL-positive cells were counted in 10 random fields from each experimental situation at 400× magnification. B: Fluorescence micrographs of tumor sections from the control mice (top field) and from the experimentals fed with 25, 50, and 75 mmol G/kg food (lower 3 fields, respectively). Left side: The arrows indicate fluorescing TUNEL-positive apoptotic cells; right side: total nuclei staining blue with DAPI. C: The activity of caspase-3 in tumor homogenates was quantified by a commercial kit as described in **Materials and Methods**, with p-nitroanilide (pNA) being the product of substrate cleavage. Values are expressed as means ± SEM, $n = 4$. $^{*}P < 0.01$; $^{***}P < 0.001$ (color figure available online).

prenyl-containing groups covalently attached to a Ras protein (through a posttranslational modification) by the farnesyl- or geranylgeranyl-transferase enzyme (30). Isoprenoids have been shown to affect these modifications (4), thus preventing the optimal functioning of the Ras. The present study demonstrated that G decreased the amount of Ras protein bound to membranes but not the total Ras-protein content of the cell, suggesting alterations in the posttranslational modification of the Ras protein through a lack of prenylation. Because depleted mevalonate levels resulted from the inhibition of HMGCR by G, that decrease in the concentration of the rate-limiting intermediate should consequently diminish the pools of farnesyl and other phosphorylated products that, for their part, are necessary for the isoprenylation of the Ras proteins. This lack of Ras prenylation would accordingly be the result of a substrate deficiency for the prenylases. In a recent report (29), however, we suggested that this effect is very likely not to be the main mechanism by which G inhibits the prenylation of certain proteins. There we hypothesized that G interfered with the incorporation of mevalonic-acid-derived products into Ras proteins by a combination of events—including

TABLE 2
Circulating cholesterol levels in tumor-bearing mice and ^{14}C incorporation into liver and tumor nonsaponifiable lipids

		^{14}C incorporation into nonsaponifiable lipids (dpm as a percent of control group)	
	Serum cholesterol (g/l)	Liver	Tumor
Control	1.073 ± 0.035	100.0 ± 18.4	100.0 ± 25.76
25 mmol G/kg food	0.954 ± 0.055	50.24 ± 5.1	66.85 ± 34.81
50 mmol G/kg food	0.852 ± 0.060*	48.32 ± 5.4	46.17 ± 16.10
75 mmol G/kg food	0.861 ± 0.051*	21.27 ± 1.4*	26.11 ± 10.44*

Cholesterolemia was determined in each animal serum by an enzymatic method as described in **Materials and Methods**. The values represent the means ± SEM, $6 \leq n \leq 20$. The radioactivity (dpm) incorporated into nonsaponifiable lipids of the mouse-host livers and the tumors were quantified. The results are expressed as the mean ± SEM with $3 \leq n \leq 5$.

*$P < 0.05$.

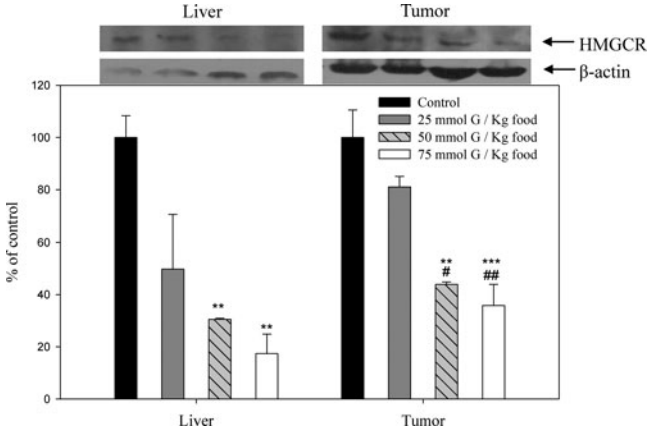

FIG. 5. The effect of geraniol on 3-hydroxymethylglutarylcoenzyme-A reductase (HMGCR) protein levels. HMGCR levels were determined in liver and tumor cells by Western blotting followed by densitometry quantitation through the use of the ImageJ software. β-actin was included in the runs as a loading control. Upper panel: HMGCR immunoblot bands. Middle panel: ß-actin–immunoblot bands. Lower panel: Density of HMGCR-immunoblot bands as a percent of the control after scanning and correction for differences in loading as described in **Materials and Methods**. Values are expressed as means ± SEM, $n = 3$. $^{**}P < 0.01$; $^{***}P < 0.001$ vs. control group. $\#P < 0.05$; $\#\#P < 0.01$ vs. group treated with 25 mmol G/kg food.

the depleted mevalonate levels, but possibly also by impairing farnesyl-protein–transferase activity (8,31). Furthermore, that several cellular lipids are fulfilling major roles in cell growth and division should also be kept in mind. Our results showed that G inhibited nonsaponifiable-lipid synthesis both in tumor cells and normal liver (Table 2), and several studies in our laboratory had previously demonstrated that cholesterol was the major nonsaponifiable lipid whose biosynthesis was inhibited by G (27–29). In addition, the higher doses of G significantly decreased the concentration of serum cholesterol in the treated mice (Table 2). This effect is consistent with recent results from this laboratory (unpublished) that indicated an increase in the expression in mouse liver and tumor cells of the mRNA encoding the plasma-membrane low-density lipoprotein receptor that binds and internalizes cholesterol from the extracellular fluid after treatment with G. We also found that G inhibited fatty-acid biosynthesis both in tumor cells and in mouse liver. Studies in culture furthermore showed that G inhibited phospholipid (e.g., phosphtidyl-choline) biosynthesis in both HepG2 (29) and A549 cells (data not shown). These results demonstrate that G clearly restricts the availability of lipids that are essential for cell growth and proliferation so as to lead to a blockade of cell growth and to apoptosis.

Apoptosis induction has been reported as the main mechanism in the anticarcinogenic action of isoprenoids (25), and G has been suggested as one of the most potent inducers (32). In addition, this effect was expected to be more pronounced in malignant cells than in normal cells (8). In keeping with this notion, we observed that G increased the amount of apoptotic cells in the A549 tumor line implanted in mice (Fig. 4) without an increase in the number of apoptotic cells in the host liver (data not shown).

Tumor-cell survival, death, and cell-cycle traverse are interconnected mechanistically (33). We recently reported that G inhibits cell-cycle progression (with an arrest occurring at the G0/G1 interphase) in Hep-G2 cells (28). We thus propose here that the mechanisms by which G could exert antitumor activity against A549 cells involve associations among all of the following actions at the molecular level: suppression of the synthesis of essential lipids for cellular growth such as fatty acids, phospholipids, cholesterol, and prenyl groups and inhibition of the relevant prenyltransferase enzymes. These effects, in turn, induce an arrest in cell-cycle progression along with a concomitant stimulation of apoptosis. Moreover, all of the antitumor effects observed in our experiments occurred at dietary doses that did not cause significant toxicity to the animals. These results accordingly point to the possibility that G could be exploited as a promising candidate for use in human lung cancer prevention and therapy with the added benefit of low toxicity.

FUNDING

This work was supported by research grants from Consejo Nacional de Investigaciones Científicas y Técnicas, Argentina Agencia Nacional de Promoción Científica y Tecnológica, and Universidad Nacional de La Plata.

We would like to thank Margarita Salas, Gabriela Finarelli, and Agustina Castro for assisting with certain experiments. We are also grateful to Dr. Donald F. Haggerty, a retired career investigator and native English speaker, for editing the final version of the manuscript. We have no conflicts of interest to declare.

REFERENCES

1. World Health Organization, Programmes and Projects: *MediaCenter: Fact Sheets*. Retrieved from http://www.who.int/mediacentre/factsheets/fs297/en/
2. Rami-Porta R, Crowley J, and Goldstraw P: Review the revised TNM staging system for lung cancer. *Ann Thorac Cardiovasc Surg* **15**, 5, 2009.
3. Goldstein JL and Brown MS: Regulation of the mevalonate pathway. *Nature* **343**, 425–430, 1990
4. Kelly M and Raymond J: Anti-cancer therapy: targeting the mevalonate pathway. *Curr Cancer Drugs Targets* **6**, 15–37, 2006.
5. Espenshade P and Adam L: Regulation of sterol synthesis in eukaryotes. *Genetics* **41**, 401–427, 2007.
6. McAnally JA, Gupta J, Sodhani S, Bravo L, and Mo H: Tocotrienols potentiate lovastatin-mediated growth suppression in vitro and in vivo. *Exp Biol Med (Maywood)* **232**, 523–531, 2007.
7. Borgquist Signe, Djerbi S, Pont F, Anagnostaki L, Goldman M, et al.: HMG_CoA reductase expression in breast cancer is associated with a less aggressive phenotype and influenced by anthropometric factors. *Int J Cancer* **123**, 1146–1153, 2008.
8. Duncan R, Lau D, El-Sohemy A, and Archer M: Geraniol and β-ionone inhibit proliferation, cell cycle progression, and cyclin-dependent kinase 2 activity in MCF-7 breast cancer cells independent of effects on HMG-CoA reductase activity. *Biochem Pharm* **68**, 1739–1747, 2004.
9. Wright L and Philips M: Thematic review series: Lipid posttranslational modifications CAAX modification and membrane targeting of Ras. *J Lipid Res* **47**, 883–891, 2006.

10. Peffley D and Gayen A: Plant-derived monoterpenes suppress hamster kidney cell 3-hydroxy-3-methylglutaryl coenzyme a reductase synthesis at the post-transcriptional level. *J Nutr* **133**, 38–44, 2003.
11. Fernandes N, Guntipalli P, and Mo H: D-δ-tocotrienol-mediated cell cycle arrest and apoptosis in human melanoma cells. *Anticancer Res* **30**, 4937–4944; 2010.
12. Greay S and Hammer K: Recent developments in the bioactivity of mono- and diterpenes: anticancer and antimicrobial activity. *Phytochem Rev* **1**, 1–6, 2011.
13. Chen W and Viljoen A: Geraniol—a review of a commercially important fragrance material. *S Afr J Bot* **76**, 643–651, 2010.
14. Mosmann T: Rapid colorimetric assay for cellular growth and survival: application to proliferation and cytotoxicity assays. *J Immunol Meth* **65**, 55–63, 1983.
15. Polo M and Bravo M: Simvastatin effects on a human lung carcinoma and cholesterol homeostasis of host and non-host mice. *Arch Physiol Biochem* **109**, 435–440, 2001.
16. Wolfensohn S and Lloyd M: *Handbook of Laboratory Animal Management and Welfare, 4th ed.*, Oxford, UK: John Wiley & Sons, 2013.
17. Folch J, Lees M, and Solane-Stanley G: A simple method for the isolation and purification of total lipids from animal tissues. *J Biol Chem* **226**, 497–509, 1957.
18. Mander E, Dean R, Stanley K, and Jessup W: Apolipoprotein B of oxidized LDL accumulates in the lysosomes of macrophages. *Biochim Biophys Acta* **1212**, 80–92, 1994.
19. Bradford M: A rapid and sensitive method for the quantitation of microgram quantities of protein utilizing the principle of protein-dye binding. *Anal Biochem* **72**, 248–254, 1976.
20. Meresman G, Olivares C, Vighi S, Alfie M, Irigoyen M, et al.: Apoptosis is increased and cell proliferation is decreased in out-of-phase endometria from infertile and recurrent abortion patients. *Reprod Biol Endocrinol* **8**, 126, 2010.
21. Stan S, Singh S, and Brand R: Chemoprevention strategies for pancreatic cancer. *Nat Rev Gastroenterol Hepatol* **7**, 347–356, 2010.
22. Carnesecchi S, Schneider Y, Ceraline J, Duranton B, Gosse F, et al.: Geraniol, a component of plant essential oils, inhibits growth and polyamine biosynthesis in human colon cancer cells. *J Pharmacol Exp Ther* **298**, 197–200, 2001.
23. Ong T, Heidor R, de Conti A, Dagli M, and Moreno F:Farnesol: and geraniol chemopreventive activities during the initial phases of hepatocarcinogenesis involve similar actions on cell proliferation and DNA damage, but distinct actions on apoptosis, plasma cholesterol and HMGCoA reductase. *Carcinogenesis* **27**, 1194–1203, 2006.
24. Manoharan S and Vasantha Selvan M: Chemopreventive potential of geraniol in 7, 12-dimethylbenz (a) anthracene (DMBA) induced skin carcinogenesis in Swiss albino mice. *J Environ Biol* **33**, 255, 2012.
25. Cardozo M, de Conti A, Ong T, Scolastici C, Purgatto E, et al.:Chemopreventive effects of β-ionone and geraniol during rat hepatocarcinogenesis promotion: distinct actions on cell proliferation, apoptosis, HMGCoA reductase, and RhoA. *J Nutr Biochem* **22**, 130–135, 2011.
26. Chaudhary S, Siddiqui M, Athar M, and Alam M: Geraniol inhibits murine skin tumorigenesis by modulating COX_2 expression, Ras_ERK1/2 signaling pathway and apoptosis. *J Appl Toxicol* **33**, 828–837, 2013.
27. Polo M and de Bravo M: Effect of geraniol on fatty-acid and mevalonate metabolism in the human hepatoma cell line Hep G2. *Biochem Cell Biol* **84**, 102–111, 2006.
28. Polo M, Crespo R, and Bravo M: Geraniol and simvastatin show a synergistic effect on a human hepatocarcinoma cell line. *Cell Biochem and Funct* **29**, 452–458, 2011.
29. Crespo R, Montero Villegas S, Abba M, de Bravo M, and Polo M: Transcriptional and posttranscriptional inhibition of HMGCR and PC biosynthesis by geraniol in 2 Hep-G2 cell proliferation linked pathways. *Biochem Cell Biol* **91**, 131–139, 2013.
30. Gysin S, Salt M, Young A, and McCormic F: Therapeutic Strategies for Targeting Ras Proteins. *Genes Cancer* **2**, 359–372, 2011.
31. Mo H and Elson C: Studies of the isoprenoid-mediated inhibition of mevalonate synthesis applied to cancer chemotherapy and chemoprevention. *Exp Biol Med (Maywood)* **229**, 567–585, 2004.
32. Shunsuke I, Osamu T, and Toshifumi H: Geraniol Is a Potent Inducer of Apoptosis-like Cell Death in the Cultured Shoot Primordia of Matricaria chamomilla. *Bioch and Bioph* **259**, 519–522, 1999.
33. Maddika S, Ande S, Panigrahi S, Paranjothy T, Weglarczyk K, et al.: Cell survival, cell death and cell cycle pathways are interconnected: implications for cancer therapy. *Drug Resist Updat* **10**, 13–29, 2007.